Analytical stability boundaries for quantum cascade lasers subject to optical feedback

Gaetan Friart,[1,*] Guy Van der Sande,[2] Guy Verschaffelt,[2] and Thomas Erneux[1]
[1]*Université libre de Bruxelles, Optique Nonlinéaire Théorique, Campus Plaine, C.P. 231, 1050 Bruxelles, Belgium*
[2]*Vrije Universiteit Brussel, Applied Physics Research Group (APHY), Pleinlaan 2, 1050 Brussel, Belgium*
(Received 19 November 2015; published 2 May 2016)

We consider nonlinear rate equations appropriate for a quantum cascade laser subject to optical feedback. We analyze the conditions for a Hopf bifurcation in the limit of large values of the delay. We obtain a simple expression for the critical feedback rate that highlights the effects of key parameters such as the linewidth enhancement factor and the pump. All our asymptotic approximations are validated numerically by using a path continuation technique that allows us to follow Hopf bifurcation points in parameter space.

DOI: 10.1103/PhysRevE.93.052201

I. INTRODUCTION

Since the original demonstration of terahertz quantum-cascade lasers (QCLs) in 2002 [1], the performance of these devices has shown rapid improvement. QCLs can now deliver milliwatts or more of continuous-wave radiation throughout the terahertz frequency range (300 GHz to 10 THz) [2]. Therefore, QCLs have become widely used in various applications such as spectroscopy, metrology, or free-space telecommunications [3]. In a QCL, the light originates from intersubband transitions rather than from electron-hole recombinations. Electron equilibration between energy subbands is dominated by phonon-assisted processes that occur on a fast picosecond timescale that contrasts to the nanosecond timescale of the carrier lifetime in conventional semiconductor lasers (SLs). As a consequence, QCLs exhibit no damped relaxation oscillations and tolerate strong optical feedback [4]. This is of particular interest because the first Hopf bifurcation instability for conventional SLs is known to exhibit sustained relaxation oscillations [5,6]. Another feature of QCLs is the fact that they exhibit low values of the linewidth enhancement factor (LEF). The LEF expresses a coupling between the amplitude and the phase of the electrical field and has a destabilizing effect for conventional SLs if its value surpasses 1 [7].

The effect of optical feedback on QCLs has recently been examined experimentally [4,8] and numerically [9,10] with the aim to determine if an oscillatory instability was possible. Results indicate that QCLs exhibit strong tolerance to optical feedback and have led to new applications such as displacement sensors [11] or terahertz imaging [12,13].

As QCLs operate out of equilibrium, a rigorous modeling requires nonequilibrium methods. Specifically, different approaches have been developed to simulate carrier transport in the nanostructured gain medium. Density matrix, Monte Carlo, and nonequilibrium Green's functions methods have led to predictive models (see review in Ref. [14]) and have achieved good agreement with experiments [15]. However, they are often too complex to detect dynamical instabilities and to explore their dependence in parameter space. Rate equations models have proven to be very efficient for semiconductor laser dynamics [16]. A three-level model developed for QCLs has been widely used by different groups (see review in Ref. [17]) and successfully describes experimental results under optical feedback [8]. It is worth noting that the parameters of such a model are sensitive to the specific design of the laser structure and may then vary for different designs in a relatively wide range of values. We have identified several sets of parameters used in the literature and verified that our conclusions on the dynamical stability of QCL subject to optical feedback remain valid for all these parameters ranges.

We propose to determine an analytical approximation of the first Hopf bifurcation that delimits the domain of stability in parameter space. All our results are validated numerically by using a path continuation technique that allows us to follow Hopf bifurcation points. Our expression for the critical feedback is simple and permits us to identify the role of the LEF and the pump current.

We consider a three-level model and we show how these rate equations can be reduced to the standard Lang and Kobayashi (LK) delay differential equations [18] for conventional SLs. In this way, we provide a link to previous analytical and numerical studies of QCLs subject to optical feedback where the LK equations have been investigated in the limit of large ratios of the photon to carrier lifetimes ($\gamma = \tau_p/\tau_c$) [4,9]. We then analyze the limit of large delay of these equations.

The plan of the paper is as follows. In Sec. II, we formulate the rate equations for two carrier populations coupled to the electrical field. Time constants for the solitary laser are well documented for this model and we show how the three equations can be reduced to the standard LK equations. We then analyze the conditions for a Hopf bifurcation and determine an asymptotic expression for the critical feedback rate. As expected, its value is significantly larger than the one for conventional SLs but could be reduced if the laser is operated close to threshold. In Sec. III, we perform systematic simulations of the original three rate equations that validate our approximations. Last, in Sec. IV, we discuss our main results. Mathematical details are relegated in the Appendix.

II. ASYMPTOTIC ANALYSIS

A. Formulation

The response of a QCL subject to a delayed feedback is analyzed using the rate equations formulated in Refs. [17,19,20] on the basis of a three level model with an extra term describing

*gfriart@ulb.ac.be

the feedback. These equations consist of a complex equation for the electric field E coupled to two real equations for carrier populations N_2 and N_3. They are given by

$$\frac{dN_3}{dt} = \frac{I_{in}}{q} - \left(\frac{1}{\tau_{32}} + \frac{1}{\tau_{31}}\right)N_3 - g(N_3 - N_2)|E|^2, \quad (1)$$

$$\frac{dN_2}{dt} = \frac{N_3}{\tau_{32}} - \frac{N_2}{\tau_{21}} + g(N_3 - N_2)|E|^2, \quad (2)$$

$$\frac{dE}{dt} = \frac{1}{2}(1 + i\alpha)\left[N_p g(N_3 - N_2) - \frac{1}{\tau_p}\right]E + \eta' \exp(-i\Omega_0\theta)E(t - \theta). \quad (3)$$

In Eqs. (1)–(3), I_{in} is the injected current into level 3, q is the electron charge, and g is the gain coefficient. The phonon scattering times between level 3 and level 2, between level 3 and level 1, and between level 2 and level 1 are denoted by τ_{32}, τ_{31}, and τ_{21}, respectively. τ_p is the photon lifetime and α is the LEF. η' is the feedback strength, θ is the delay of the feedback, and $\Omega_0\theta$ is the feedback phase. From Eqs. (1)–(3) we formulate in the Appendix dimensionless equations for the dimensionless electric field Y' and carriers V and Z. They are given by Eqs. (A16)–(A18) in the Appendix and are of the form

$$\frac{dZ}{ds} = \gamma_1[P - \gamma_4 Z + \gamma_3 V - (1 + 2Z)2|Y'|^2], \quad (4)$$

$$\frac{dV}{ds} = \gamma_2[2Z - V + (1 + 2Z)2|Y'|^2], \quad (5)$$

$$\frac{dY'}{ds} = (1 + i\alpha)ZY' + \eta \exp(-i\omega_0\tau)Y'(s - \tau), \quad (6)$$

where time s is measured in units of the photon lifetime. P is the renormalized pump parameter above threshold, τ is the delay, and γ_1, γ_2, γ_3, and γ_4 are dimensionless combinations of phonon scattering times defined in the Appendix. Based on typical values of the time constants, it was shown in Ref. [17] that we may eliminate adiabatically one variable from Eqs. (4)–(6). We follow the same approach and explain the adiabatic elimination in the Appendix.

Introducing then $Z = \frac{1}{2}(N - 1)$ into Eqs. (A25) and (A26) to be consistent with the notation of Ref. [9] leads to the following LK equations [16,18]:

$$\frac{dY}{ds} = \frac{1}{2}(1 + i\alpha)(N - 1)Y + \eta \exp(-i\omega_0\tau)Y(s - \tau), \quad (7)$$

$$\frac{dN}{ds} = \gamma[I - N(1 + |Y|^2)], \quad (8)$$

where $I \equiv P/A + 1$, $\gamma \equiv 2\gamma_1 A$ and $A \equiv \frac{1}{2}(\gamma_4 - 2\gamma_3)$. We note from the last column of Table II in Ref. [17] that A is ranging from 0.6 to 1.1. The parameters of the full model associated with the intersubband transitions now appear through this parameter A. γ is an $O(1)$ fixed parameter ranging from 0.8 to 19 (see Table II in Ref. [17]). It marks the main difference with the conventional SL where γ is typically an $O(10^{-3})$ small quantity. The linear stability analysis of the nonzero intensity solution $(|Y|, N) = (\sqrt{I - 1}, 1)$ indicates a purely exponential decay if $\gamma > \gamma_{\text{th}} \equiv 4(I - 1)I^{-2}$. Since $I > 1$, γ_{th} has its maximal value at $I = 2$ and is given by $\gamma_{\text{th}} = 1$. Damped relaxation oscillations are therefore not possible if $\gamma > 1$.

In Ref. [9], $\theta \simeq 1$ ns and $\tau_p = 37.4$ ps give $\tau \simeq 30$; in Ref. [10], $\tau_p = 4.74$ ps and $\theta = 1 - 6.3$ ns lead to $\tau =$ 200–1300. Both estimates motivate exploring the limit of large delay. To this end, we first determine the external cavity modes (ECMs) and then the conditions for a Hopf bifurcation. These conditions are transcendental equations which we analyze in the limit $\tau \to \infty$.

Recent studies [4] have shown that the first dynamical instabilities in QCLs appear at relatively high feedback rate. The LK equations with a unique feedback term are valid in the limit of small rates [18], although they have shown to provide good qualitative agreement with experiments at higher feedback rates [16]. Several strategies have been developed to improve the LK model, for example, by adding multiple reflection terms in the field equation [21]. For QCLs subject to optical feedback, recent experiments have shown that the LK equations correctly predict the first oscillatory instability [4,8,22]. Nevertheless, we may check that our model remains consistent. It has indeed been pointed out that the LK equations lose their consistency when the external reflectivity exceeds the Fresnel reflectivity of the laser facets [23,24]. Following the strategy of [24], we can estimate this validity limit around $\eta = 0.5$ in our dimensionless units. The values of η considered in the next sections are below this limit.

B. ECMs and Hopf bifurcation

Introducing the decomposition $Y = R\exp(-i\omega_0 s + i\phi)$, we reformulate Eqs. (7) and (8) as

$$\frac{dR}{ds} = \frac{1}{2}(N - 1)R + \eta R(s - \tau)\cos[\phi(s - \tau) - \phi], \quad (9)$$

$$\frac{d\phi}{ds} = \omega_0 + \frac{1}{2}(N - 1)\alpha + \eta\frac{R(s - \tau)}{R}\sin[\phi(s - \tau) - \phi], \quad (10)$$

$$\frac{dN}{ds} = \gamma[I - N(1 + R^2)]. \quad (11)$$

The basic solutions are the ECMs with $\phi = \omega s$ and R and N constants. With the feedback rate η as the control parameter, they are given by (in parametric form)

$$\eta = -\frac{\omega - \omega_0}{[\alpha\cos(\omega\tau) + \sin(\omega\tau)]}, \quad (12)$$

$$R^2 = I[1 - 2\eta\cos(\omega\tau)]^{-1} - 1 \geqslant 0, \quad (13)$$

$$N = \frac{I}{1 + R^2}. \quad (14)$$

A necessary condition for stability is [25]

$$\eta\tau F + 1 > 0, \quad (15)$$

where

$$F \equiv \cos(\omega\tau) - \alpha\sin(\omega\tau). \quad (16)$$

Condition Eq. (15) was derived in Ref. [25] in the limit of small values of η [more precisely, $\eta = O(\tau^{-1})$ as $\tau \to \infty$] when the response of the laser can be described by its phase

only. The unstable branches of ECMs for which Eq. (15) is not satisfied, are called "antimodes." The branches of ECMs satisfying Eq. (15) are called "modes."

To find if a Hopf bifurcation may destabilize a stable ECM, we determine the characteristic equation for the growth rate λ. By inserting $\lambda = i\sigma$ and separating the real and imaginary parts, we obtain the following conditions for a Hopf bifurcation:

$$\begin{aligned}
&-\sigma^2[\gamma(1+R^2) - 2\eta\cos(\omega\tau)(\cos(\sigma\tau)-1)] \\
&+\sigma\begin{bmatrix}\eta^2 2(\cos(\sigma\tau)-1)\sin(\sigma\tau) \\ -\gamma(1+R^2)2\eta\cos(\omega\tau)\sin(\sigma\tau)\end{bmatrix} \\
&+\gamma(1+R^2)\eta^2[(\cos(\sigma\tau)-1)^2 - \sin^2(\sigma\tau)] \\
&-\gamma\frac{IR^2}{1+R^2}\eta(\cos(\sigma\tau)-1)F = 0 \qquad (17)\\
&-\sigma^3 - \sigma^2 2\eta\cos(\omega\tau)\sin(\sigma\tau) \\
&+\sigma\begin{bmatrix}\eta^2[(\cos(\sigma\tau)-1)^2 - \sin^2(\sigma\tau)] \\ -\gamma(1+R^2)2\eta\cos(\omega\tau)(\cos(\sigma\tau)-1) + \gamma\frac{IR^2}{1+R^2}\end{bmatrix} \\
&-\gamma(1+R^2)\eta^2 2(\cos(\sigma\tau)-1)\sin(\sigma\tau) \\
&+\gamma\frac{IR^2}{1+R^2}\eta\sin(\sigma\tau)F = 0. \qquad (18)
\end{aligned}$$

Together with Eqs. (12) and (13), they provide the values of $\omega\tau$ and σ at a Hopf bifurcation point. We have verified that these equations correctly match the conditions derived in Ref. [9] in the limit γ large. However, we are interested in solutions of these equations for $O(1)$ values of γ. In order to progress analytically, we propose an asymptotic solution based on the limit $\tau \to \infty$. A preliminary analysis assuming $\omega\tau$, $\sigma\tau$, and $\eta\tau$ as $O(1)$ quantities indicate that a solution is possible only if $\sigma = 0$. This means that a Hopf bifurcation is not possible if η is $O(\tau^{-1})$ small and that we need to consider the case η as an $O(1)$ quantity. Assuming now $\omega\tau$, $\sigma\tau$, and η as $O(1)$ quantities, we note from Eqs. (17) and (18) that the leading terms require $\sin(\sigma\tau) = 0$ and $\cos(\sigma\tau) - 1 = 0$. They imply that $\sigma\tau = 2n\pi$ where n is an integer. To determine the critical feedback rate for a Hopf bifurcation, we seek a solution of Eqs. (17) and (18) of the form

$$\sigma\tau = 2n\pi + \tau^{-1}x_1 + \tau^{-2}x_2 + \cdots. \qquad (19)$$

The leading equations are $O(\tau^{-2})$ for Eq. (17) and $O(\tau^{-1})$ for Eq. (18). They are given by

$$-(2n\pi)^2 - 4n\pi\eta\cos(\omega\tau)x_1 - \eta^2 x_1^2 + \frac{IR^2}{(1+R^2)^2}\eta\frac{x_1^2}{2}F = 0, \qquad (20)$$

$$2n\pi + \eta x_1 F = 0. \qquad (21)$$

A first observation is that γ does not appear in the leading Hopf condition Eqs. (20) and (21). To determine its effect, we need the scaling $\gamma = O(\tau^{-2}) << 1$, which is not physical for the QCL. This is consistent with the results of Ref. [4], where it is numerically anticipated that the critical feedback rate is essentially independent of γ for $\gamma > 1$. Solving Eq. (21) for x_1, we obtain

$$x_1 = -\frac{2n\pi}{\eta F}. \qquad (22)$$

Introducing then Eq. (22) into Eq. (20), we find

$$-1 + \frac{2\cos(\omega\tau)}{F} - \frac{1}{F^2} + \frac{IR^2}{(1+R^2)^2}\frac{1}{2\eta F} = 0, \qquad (23)$$

where we note that n has disappeared. This means that all the Hopf bifurcations for a given ECM collapses to the first one ($n = 1$), in first approximation as $\tau \to \infty$.

The assumption that $\omega\tau$ and η are $O(1)$ quantities leads to another important simplification. From Eq. (12), the scalings of $\omega\tau$ and η imply that the denominator is $O(\tau^{-1})$ small, or equivalently, $\alpha\cos(\omega\tau) + \sin(\omega\tau) = 0$. The ECM frequencies $\omega\tau$ thus satisfy

$$\tan(\omega\tau) = -\alpha. \qquad (24)$$

Two solutions are possible but only one satisfies Eq. (15). The expressions of $\sin(\omega\tau)$ and $\cos(\omega\tau)$ are needed for evaluating the coefficients in Eq. (23). By using Eq. (24), we find

$$\sin(\omega\tau) = -\frac{\alpha}{\sqrt{1+\alpha^2}} \text{ and } \cos(\omega\tau) = \frac{1}{\sqrt{1+\alpha^2}}. \qquad (25)$$

Using Eq. (13), we may eliminate R^2 in Eq. (23) and reformulate the Hopf condition as a linear equation for I. Using Eq. (25) and simplifying, we obtain $I = I(\eta)$ as

$$I = \frac{1}{1 - 2\eta\sqrt{\alpha^2+1}}\left(1 - \frac{2\eta}{\sqrt{1+\alpha^2}}\right)^2, \qquad (26)$$

where we recall that $I = P/A + 1$. The function $\eta = \eta(I)$ increases from $I = 1$ and saturates at $\eta = \eta_{\max}$ as $I \to \infty$, where

$$\eta_{\max} = \frac{1}{2\sqrt{\alpha^2+1}}. \qquad (27)$$

We may also determine an expression for η as a function of α (I fixed). Specifically, we formulate from Eq. (23) a quadratic equation for η, which we solve. The solution is

$$\eta_\pm = \frac{\sqrt{1+\alpha^2}}{4}[2 - (1+\alpha^2)I \pm \sqrt{(1+\alpha^2)^2 I^2 - 4I\alpha^2}]. \qquad (28)$$

If $I < 1$ and $\alpha < 1$, both solutions are real and positive in a fixed interval $I_c \leqslant I \leqslant 1$. If $I > 1$, η_+ is the only positive solution. It approaches $\eta = 1/2$ as $\alpha \to 0$, whatever the value of $I > 1$.

We illustrate and discuss our results in the next section.

III. NUMERICAL SIMULATIONS

In order to discuss the validity of our asymptotic approximations, we have determined numerically the Hopf bifurcation points from the original equations. Specifically we consider the dimensionless Eqs. (4)–(6). We progressively increase the feedback level to detect the first Hopf bifurcation destabilizing the continuous wave output of the laser. We then use a path continuation technique to follow this Hopf bifurcation in parameter space. Although our analysis is valid for arbitrary values of the feedback phase, we limit our

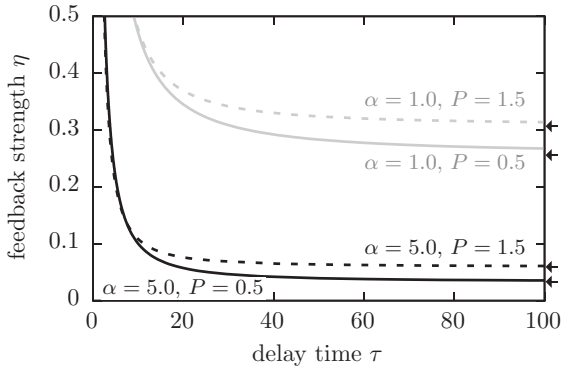

FIG. 1. Critical feedback strength η_{Hopf} as a function of the delay τ obtained by path continuation of Eqs. (4)–(6) for different values of the LEF α and the pump P. The values of the fixed parameters are $\gamma_1 = 2.75$, $\gamma_2 = 16.49$, $\gamma_3 = 0.35$, $\gamma_4 = 2.81$, and $\omega_0\tau = 0 \pmod{2\pi}$. When the delay increases, η_{Hopf} decreases and progressively reaches a constant plateau. The analytical approximation Eq. (28) of the Hopf bifurcation point (indicated by the arrows) in the large delay limit provides the value of this plateau.

numerical investigations to the case $\omega_0\tau = 0$ because it has little effects if the delay is large (see Sec. II.D.1. in Ref. [26]).

We first analyze how the critical feedback strength η_{Hopf}, given by η in Eq. (26) or η_+ in Eq. (28), depends on the delay τ of the feedback; see Fig. 1. At small delay times, the Hopf bifurcation appears at high feedback rates, for which the rate equations considering only a single reflection are no more valid. Moreover these high feedback rates are hard to reach experimentally. The laser output is consequently stable for small delays and a broad range of feedback strength. When the delay increases, η_{Hopf} decreases and progressively reaches a constant plateau. The asymptotic Eq. (28) of the Hopf bifurcation in the large delay limit provides this constant plateau, indicated by the arrows in Fig. 1. Depending on the particular values of P and α, the asymptotic approximation becomes good for values of the delay between 100 and 500. A dimensionless delay of 100 corresponds to an external cavity length of a few centimeters.

We compare our Eq. (26) of η_{Hopf} as a function of the pump with the numerical results obtained by the path continuation

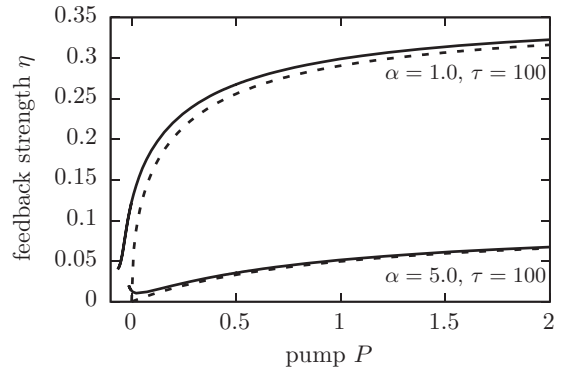

FIG. 2. Critical feedback strength η_{Hopf} as a function of the pump parameter P for $\alpha = 1$ and $\alpha = 5$ ($\tau = 100$). The continuous lines are the numerical continuations of the bifurcation point while the dashed lines correspond to the asymptotic Eq. (26). Same values of the fixed parameters as described in the caption of Fig. 1.

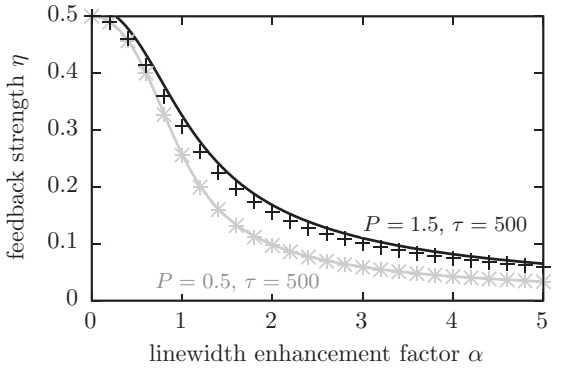

FIG. 3. Critical feedback strength η_{Hopf} as a function of the LEF α for $P = 0.5$ and $P = 1.5$ ($\tau = 500$). The continuous lines are the numerical results obtained by the path continuation of the bifurcation point while the marks denote the asymptotic values obtained from Eq. (28). Quantitative agreement is observed for $\tau = 500$.

method in Fig. 2. The figure shows that, already for $\tau = 100$, Eq. (26) reproduces well the main trend of the curve and is in good quantitative agreement for large values of α. Only as $P \to 0$, the approximation of the Hopf bifurcation point in terms of the feedback rate progressively fails because $\eta \to 0$ contradicts our basic assumption $\eta = O(1)$.

In Fig. 2, the exact numerical bifurcation lines (continuous lines) continue to small negative values of the pump. This is possible because the feedback reduces the threshold. From Eq. (13) with $R = 0$ and using Eq. (25), we find that the threshold current is given by

$$I_{\text{th}} = 1 - \frac{2\eta}{\sqrt{1+\alpha^2}}. \tag{29}$$

This reduction was verified experimentally in [10].

Moreover, Eq. (28) indicates that two Hopf bifurcations are possible below $P = 0$ if $\alpha^2 < 1$. To further study this case a new analysis where both η and $I - 1$ are scaled with respect to τ^{-1} will be needed.

Finally, we discuss the influence of the linewidth enhancement factor α on the stability of the laser output. Figure 3 shows η_{Hopf} as a function of α for a large delay ($\tau = 500$). Our asymptotic approximation is in good agreement with the numerical results. As expected, α has a destabilizing effect. This corroborates the similar conclusions obtained using the conventional LK model for the QCL in Ref. [9].

IV. CONCLUSION

In this paper, we show how the three level rate equations for a QCL subject to feedback reduce to the LK equations. We derive an asymptotic expression of the Hopf bifurcation point destabilizing the steady intensity valid in the limit of large delay. Using the full three level model, we determine numerically the Hopf bifurcation point in parameter space by using a continuation technique. As the delay is increased, the critical feedback rate progressively reaches a constant value, which substantiates our asymptotic results. A QCL laser with small LEF is more tolerant to optical feedback. Moreover, increasing the pump current increases the critical feedback strength. For a conventional semiconductor laser, η_{Hopf} is

generally an $O(10^{-3})$ quantity [16]. For a QCL η_{Hopf} is an $O(10^{-1})$ quantity but could be reduced if the laser is closed to threshold (P small). This is indeed the strategy followed in Ref. [22] to find experimental evidence of pulsating instabilities. The scaling law between the critical feedback and the pump parameter can be found by expanding Eq. (26) for small η. We find that η is proportional to P for small P and $\alpha > 1$.

ACKNOWLEDGMENTS

G.F. acknowledges the support of the Belgian Fonds pour la Formation à la Recherche dans l'Industrie et dans l'Agriculture (FRIA) GVdS and GV acknowledge support from the FWO-project "Widely tunable quantum cascade lasers based on filtered feedback through III/V silicon hybrid integration." T.E. acknowledges the support of the Fonds de la Recherche Scientifique (FNRS) (Belgium). This work benefited from the support of the Belgian Science Policy Office under Grant No. IAP-7/35 "photonics@be."

APPENDIX

Starting from Eqs. (1)–(3), we first introduce the new time $s \equiv t/\tau_p$ and the new variable $N \equiv N_3 - N_2$. The later is motivated by the fact that $N_3 - N_2$ appears in all three equations. We rewrite Eqs. (1)–(3) in terms of s, N, N_2, and ϕ and obtain

$$\frac{1}{\tau_p}\frac{dN}{ds} = \frac{I_{\mathrm{in}}}{q} - \left(\frac{2}{\tau_{32}} + \frac{1}{\tau_{31}}\right)N - 2gN|E|^2 + \left[\frac{1}{\tau_{21}} - \left(\frac{2}{\tau_{32}} + \frac{1}{\tau_{31}}\right)\right]N_2, \tag{A1}$$

$$\frac{1}{\tau_p}\frac{dN_2}{ds} = \frac{N}{\tau_{32}} - \left(\frac{1}{\tau_{21}} - \frac{1}{\tau_{32}}\right)N_2 + gN|E|^2, \tag{A2}$$

$$\frac{dE}{ds} = \frac{1}{2}(1+i\alpha)[\tau_p N_p g N - 1]E + \eta'\tau_p \exp(-i\Omega_0\theta)E(s-\theta/\tau_p). \tag{A3}$$

Second, the expression in brackets in Eq. (A3) motivates us to rename N so that this expression can be reduced to a single term. Specifically, we introduce the new variable Z as

$$N = \frac{1+2Z}{N_p g \tau_p}. \tag{A4}$$

We then obtain

$$\frac{2\tau_{32}}{N_p g \tau_p^2}\frac{dZ}{ds} = \frac{I_{\mathrm{in}}\tau_{32}}{q} - \left(2 + \frac{\tau_{32}}{\tau_{31}}\right)\frac{1+2Z}{N_p g \tau_p} + \left[\frac{\tau_{32}}{\tau_{21}} - \left(2 + \frac{\tau_{32}}{\tau_{31}}\right)\right]N_2 - 2g\tau_{32}\frac{1+2Z}{N_p g\tau_p}|E|^2, \tag{A5}$$

$$\frac{\tau_{32}}{\tau_p}\frac{dN_2}{ds} = \frac{1+2Z}{N_p g \tau_p} - \left(\frac{\tau_{32}}{\tau_{21}} - 1\right)N_2 + \tau_{32} g \frac{1+2Z}{N_p g \tau_p}|E|^2, \tag{A6}$$

$$\frac{dE}{ds} = (1+i\alpha)ZE + \eta'\tau_p \exp(-i\Omega_0\theta)E(s-\theta/\tau_p). \tag{A7}$$

Third, the laser threshold of the solitary laser corresponds to $Z = |E| = 0$. From Eq. (A6) at steady state, this then implies that $N_2 = [N_p g \tau_p (\frac{\tau_{32}}{\tau_{21}} - 1)]^{-1}$. This expression motivates introducing the new variable V as

$$N_2 = \frac{1}{N_p g \tau_P}\frac{1+V}{\left(\frac{\tau_{32}}{\tau_{21}} - 1\right)}. \tag{A8}$$

Inserting Eq. (A8) into Eqs. (A5)–(A7), we obtain

$$\frac{2\tau_{32}}{N_p g \tau_p^2}\frac{dZ}{ds} = \frac{I_{\mathrm{in}}\tau_{32}}{q} - \left(2 + \frac{\tau_{32}}{\tau_{31}}\right)\frac{1+2Z}{N_p g\tau_p} + \left[\frac{\tau_{32}}{\tau_{21}} - \left(2 + \frac{\tau_{32}}{\tau_{31}}\right)\right]\frac{1}{N_p g \tau_P}\frac{1+V}{\left(\frac{\tau_{32}}{\tau_{21}} - 1\right)} - 2g\tau_{32}\frac{1+2Z}{N_p g\tau_p}|E|^2, \tag{A9}$$

$$\frac{\tau_{32}\left(\frac{\tau_{32}}{\tau_{21}} - 1\right)^{-1}}{N_p g \tau_P^2}\frac{dV}{ds} = \frac{1+2Z}{N_p g\tau_p} + \tau_{32} g \frac{1+2Z}{N_p g\tau_p}|E|^2 - \left(\frac{\tau_{32}}{\tau_{21}} - 1\right)\frac{1}{N_p g\tau_P}\frac{1+V}{\left(\frac{\tau_{32}}{\tau_{21}} - 1\right)}, \tag{A10}$$

$$\frac{dE}{ds} = (1+i\alpha)ZE + \eta'\tau_p \exp(-i\Omega_0\theta)E(s-\theta/\tau_p). \tag{A11}$$

Simplifying,

$$\frac{dZ}{ds} = \frac{\tau_p}{\tau_{32}}\begin{bmatrix} \frac{N_p g\tau_p}{2}\frac{I_{in}\tau_{32}}{q} \\ -\left(2+\frac{\tau_{32}}{\tau_{31}}\right)\frac{1}{2} - \left(2+\frac{\tau_{32}}{\tau_{31}}\right)Z \\ +\left[\frac{\tau_{32}}{\tau_{21}} - \left(2+\frac{\tau_{32}}{\tau_{31}}\right)\right]\frac{1}{2}\frac{1}{\left(\frac{\tau_{32}}{\tau_{21}}-1\right)} \\ +\left[\frac{\tau_{32}}{2\tau_{21}} - \left(1+\frac{\tau_{32}}{2\tau_{31}}\right)\right]\frac{V}{\left(\frac{\tau_{32}}{\tau_{21}}-1\right)} \\ -g\tau_{32}(1+2Z)|E|^2 \end{bmatrix}, \tag{A12}$$

$$\frac{dV}{ds} = \frac{\tau_p}{\tau_{32}}\left(\frac{\tau_{32}}{\tau_{21}} - 1\right)\begin{bmatrix} 2Z - V \\ +\tau_{32} g(1+2Z)|E|^2 \end{bmatrix}, \tag{A13}$$

$$\frac{dE}{ds} = (1+i\alpha)ZE + \eta'\tau_p \exp(-i\Omega_0\theta)E(s-\theta/\tau_p), \tag{A14}$$

and introducing

$$Y' = \sqrt{\frac{g\tau_{32}}{2}}E, \tag{A15}$$

we obtain

$$\frac{dZ}{ds} = \gamma_1[P - \gamma_4 Z + \gamma_3 V - (1+2Z)2|Y'|^2], \tag{A16}$$

$$\frac{dV}{ds} = \gamma_2[2Z - V + (1+2Z)2|Y'|^2], \tag{A17}$$

$$\frac{dY'}{ds} = (1+i\alpha)ZY' + \eta \exp(-i\omega_0\tau)Y'(s-\tau). \tag{A18}$$

The parameters γ_1, γ_2, γ_3, γ_4, P, η, τ, and ω_0 are defined by

$$\gamma_1 = \frac{\tau_p}{\tau_{32}}, \quad \gamma_2 = \left(\frac{\tau_{32}}{\tau_{21}} - 1\right)\frac{\tau_p}{\tau_{32}}, \tag{A19}$$

$$\gamma_3 = \left(\frac{\tau_{32}}{2\tau_{21}} - 1 - \frac{\tau_{32}}{2\tau_{31}}\right)\frac{1}{\left(\frac{\tau_{32}}{\tau_{21}} - 1\right)}, \tag{A20}$$

$$\gamma_4 = 2\left(1 + \frac{\tau_{32}}{2\tau_{31}}\right), \quad P \equiv \frac{N_p g \tau_p \tau_{32}}{2}\frac{I_{in} - I_{th}}{q}, \tag{A21}$$

$$\eta = \eta'\tau_p, \quad \tau = \theta/\tau_p, \quad \omega_0 = \Omega_0\tau_p. \tag{A22}$$

The threshold current satisfies

$$\frac{N_p g \tau_p \tau_{32}}{2}\frac{I_{th}}{q} - \left(1 + \frac{\tau_{32}}{2\tau_{31}}\right) + \left(\frac{\tau_{32}}{2\tau_{21}} - 1 - \frac{\tau_{32}}{2\tau_{31}}\right)\frac{1}{\left(\frac{\tau_{32}}{\tau_{21}} - 1\right)} = 0. \tag{A23}$$

The large value of γ_2 [17] suggests to eliminate V by a quasi-steady-state approximation. Equation (A17) then gives

$$V = 2Z + 2(1 + 2Z)|Y'|^2. \tag{A24}$$

The remaining equations are now of the form

$$\frac{dZ}{ds} = \frac{1}{2}\gamma_1(\gamma_4 - 2\gamma_3)[P' - 2Z - (1 + 2Z)|Y|^2], \tag{A25}$$

$$\frac{dY}{ds} = (1 + i\alpha)ZY + \eta\exp(-i\omega_0\tau)Y(s - \tau), \tag{A26}$$

where $Y = 2\sqrt{\frac{1-\gamma_3}{\gamma_4 - 2\gamma_3}}Y'$ and $P' = \frac{2P}{\gamma_4 - 2\gamma_3}$.

[1] R. Köhler, A. Tredicucci, F. Beltram, H. E. Beere, E. H. Linfield, A. G. Davies, D. A. Ritchie, R. C. Iotti, and F. Rossi, Nature **417**, 156 (2002).

[2] B. S. Williams, Nat. Photonics **1**, 517 (2007).

[3] M. S. Vitiello, G. Scalari, B. Williams, and P. D. Natale, Opt. Express **23**, 5167 (2015).

[4] F. P. Mezzapesa, L. L. Columbo, M. Brambilla, M. Dabbicco, S. Borri, M. S. Vitiello, H. E. Beere, D. A. Ritchie, and G. Scamarcio, Opt. Express **21**, 13748 (2013).

[5] M. Wolfrum and D. Turaev, Opt. Commun. **212**, 127 (2002).

[6] G. Friart, L. Weicker, J. Danckaert, and T. Erneux, Opt. Express **22**, 6905 (2014).

[7] A. M. Levine, G. H. M. van Tartwijk, D. Lenstra, and T. Erneux, Phys. Rev. A **52**, R3436 (1995).

[8] L. Jumpertz, M. Carras, K. Schires, and F. Grillot, Appl. Phys. Lett. **105**, 131112 (2014).

[9] L. L. Columbo and M. Brambilla, Opt. Express **22**, 10105 (2014).

[10] L. Jumpertz, S. Ferré, K. Schires, M. Carras, and F. Grillot, Proc. SPIE **9370**, Quantum Sensing and Nanophotonic Devices XII, 937014 (2015).

[11] Y. Leng Lim, P. Dean, M. Nikolić, R. Kliese, S. P. Khanna, M. Lachab, A. Valavanis, D. Indjin, Z. Ikonić, P. Harrison, E. H. Linfield, A. Giles Davies, S. J. Wilson, and A. D. Rakić, Appl. Phys. Lett. **99**, 081108 (2011).

[12] P. Dean, A. Valavanis, J. Keeley, K. Bertling, Y. L. Lim, R. Alhathlool, A. D. Burnett, L. H. Li, S. P. Khanna, D. Indjin, T. Taimre, A. D. Rakić, E. H. Linfield, and A. G. Davies, J. Phys. D: Appl. Phys. **47**, 374008 (2014).

[13] J. Keeley, P. Dean, A. Valavanis, K. Bertling, Y. L. Lim, R. Alhathlool, T. Taimre, L. H. Li, D. Indjin, A. D. Rakić, E. H. Linfield, and A. G. Davies, Opt. Lett. **40**, 994 (2015).

[14] C. Jirauschek and T. Kubis, Appl. Phys. Rev. **1**, 011307 (2014).

[15] T. Schmielau and M. F. Pereira, Appl. Phys. Lett. **95**, 231111 (2009).

[16] T. Erneux and P. Glorieux, *Laser Dynamics* (Cambridge University Press, Cambridge, UK, 2010).

[17] T. Erneux, V. Kovanis, and A. Gavrielides, Phys. Rev. E **88**, 032907 (2013).

[18] R. Lang and K. Kobayashi, IEEE J. Quantum Electron. **16**, 347 (1980).

[19] T. Gensty, W. Elsäßer, and C. Mann, Opt. Express **13**, 2032 (2005).

[20] T. Gensty and W. Elsäßer, Opt. Commun. **256**, 171 (2005).

[21] L. N. Langley, K. A. Shore, and J. Mork, Opt. Lett. **19**, 2137 (1994).

[22] L. Jumpertz, K. Schires, M. Carras, M. Sciamanna, and F. Grillot, Light Sci. Appl. (to be published).

[23] A. A. Duarte and H. G. Solari, Phys. Rev. A **58**, 614 (1998).

[24] D. Lenstra, G. Vemuri, and M. Yousefi, *Generalized Optical Feedback: Theory, in Unlocking Dynamical Diversity: Optical Feedback Effects on Semiconductor Lasers*, edited by D. M. Kane and K. A. Shore (John Wiley & Sons, Chichester, UK, 2005).

[25] G. Acket, D. Lenstra, A. Den Boef, and B. Verbeek, IEEE J. Quantum Electron. **20**, 1163 (1984).

[26] M. C. Soriano, J. García-Ojalvo, C. R. Mirasso, and I. Fischer, Rev. Mod. Phys. **85**, 421 (2013).